Vol. 76: 59–72, 2018
https://doi.org/10.3354/cr01528

CLIMATE RESEARCH
Clim Res

Published online September 4

Projection of frequency and intensity of extreme precipitation in Zambia: a CMIP5 study

Brigadier Libanda[1,*], Chilekana Ngonga[2]

[1]School of Geosciences, The University of Edinburgh, Edinburgh, EH9 3FF, UK
[2]Ministry of Energy and Water Development, PO Box 53930, Lusaka, Zambia

ABSTRACT: Extreme precipitation exerts damaging impacts on both society and ecosystems. Understanding projections of extreme precipitation is part of a resilient response to its impacts. To avoid the generalities inherent in regional projections, projections focussing on an individual country are necessary. However, studies focusing on Zambia are still limited and future climate variability is poorly understood. Here, the frequency and intensity of extreme precipitation over Zambia are analysed for the period 2021–2100 using an ensemble of 5 CMIP5 models from those recommended by the Intergovernmental Panel on Climate Change (IPCC). Our analyses demonstrate that there will be an increase in precipitation intensity and a decrease in frequency over Zambia from the middle of the 21st century. Notably, there is a significant increase in the maximum number of consecutive dry days and significant decreases in the number of days with at least 1 and 10 mm of precipitation. Annual total precipitation significantly reduces while the frequency of exceedance of the 95th and 99th percentile thresholds increases significantly. The annual maxima of 1 d and consecutive 5 d precipitation are also projected to increase. Results from the spatial analysis show that the greatest increase in the number of consecutive dry days is around Siavonga, Kasama and Isoka, up to the border of Zambia and Tanzania. The reduction in precipitation is projected to be steepest over Northwestern Province and lessens southwards. The steepness of these trends generally falls between −0.22 and 0.47 on Sen's slope estimator at a significance level of 5%. In nearly all cases the risk of rejecting the null hypothesis H_0 when it is true is lower than 1%. Our study provides a novel overview of expected climate trends in Zambia, which can act as guidelines for strategic planning of flood and drought prevention.

KEY WORDS: Precipitation · Intensity · Frequency · Projections · CMIP5 · Zambia

1. INTRODUCTION

Precipitation is one of the most important meteorological variables, especially in developing countries where economies are mainly dependant on rain-fed agriculture (Nangombe et al. 2018). Other climate-sensitive sectors like water resources, transport and health are also dependent on the proper understanding of precipitation variability. Many studies (e.g. Davis 2011, Reason 2016) have described the climate over southern Africa as semi-arid. Precipitation varies in time and space, but the region generally experiences its main rains from October/November to March/April (Hachigonta & Reason 2006). From April to October, the region is generally dry. Thus, the rainfall pattern is best described as unimodal (Reason 2016).

Extremes in precipitation, whether positive (floods) or negative (drought), tend to cause havoc in socio-economic sectors. In a study on climate extremes over southern Africa, New et al. (2006) noted that there has been an increase in precipitation extremes across the broader southern African region in recent years. Recently, 44 people were feared dead and 79 000 were displaced across south-central Mozambique following the extreme precipitation of January

*Corresponding author: brigadier.libanda@ed.ac.uk

2017 (ReliefWeb 2017). During the same season, over 35 000 people were documented as having been affected in neighbouring Malawi (ACT Alliance 2017). Just before the close of the 2017 rainy season, Zimbabwe also experienced severe flooding across 37 districts which damaged infrastructure and halted transportation (ACAPS 2017). As a part of southern Africa, Zambia also suffers the impacts of extreme precipitation. In fact, it has been shown that 3 quarters of all disasters prevalent in Zambia are associated with extreme events (Republic of Zambia [RoZ] 2008, Libanda et al. 2015a). In a study on the impacts of climate change on economies, Chinowsky et al. (2015) found that the impact of extreme climate events in Zambia is twice that experienced by neighbouring Malawi and Mozambique. This therefore makes studies on climate extremes in Zambia necessary.

Climate extremes are one of the 'Grand Challenges' proposed by the World Climate Research Programme (WCRP) and documented by the World Meteorological Organization (WMO; Zhang et al. 2014). This is because climate extremes—extreme rainfall, extreme drought, extreme cold spells, or even extreme heat waves—invariably lead to agricultural losses, properties and houses being swept away leaving people homeless and sometimes loss of life. Therefore, studies focussing on understanding and projecting the spatio-temporal variability of climate extremes around the globe have become necessary. However, climate change increases uncertainty in understanding extremes (IPCC 2012), especially over Africa, where models generally have difficulties capturing the variations of atmospheric convection in space and time (Pohl et al. 2017). Current evidence shows that with climate change, the occurrence of extremes is equally changing (IPCC 2014). Climate change will also cause more intense storms and sea level rise (IPCC 2001) because of thermal expansion of the oceans and melting ice in the Antarctic and Arctic regions, thereby posing major challenges for coastal cities (IPCC 2013). In fact, projections show that sea level rise will still occur even if global temperatures do not cross the 2°C suggested by many scientists as a reasonable target. This has been described further by Hansen et al. (2016) who simulated the rate of sea level rise in comparison to the pre-industrial state.

With the use of climate models, climate variability and change has become an active area of research around the world in recent years, and this has led to significant discoveries and advances in climate change science. For example, Mason & Joubert (1997) used models to study changes in extreme rainfall over the broader southern African region and found that a doubling of CO_2 can lead to an increase in extreme precipitation owing to the sensitivity of convection to a rise in temperature. Engelbrecht et al. (2013) also used modelling to investigate the influence of anthropogenic forcing on closed-lows and extreme rainfall events over the broader southern African region. Their findings highlighted an increase in extreme rainfall and a downward trend in the frequencies of closed lows. The increase in extreme rainfall was attributed to the formation of cloud bands following intense convection.

Climate models generally employ mathematical formulae to simulate the dynamics of the climate system (Kaplan 2009). The relationships of the atmosphere, land surface, oceans, etc., are accounted for in climate models (Lorenz et al. 2012) to give a balanced representation of the climate system and/or to make projections. The official international voice (the Intergovernmental Panel on Climate Change, IPCC) on all matters relating to climate change documents that climate dynamics can be simulated using different representative concentration pathways (RCPs; IPCC 2014). These RCPs describe 4 different possible future climate states which depend on the amount of greenhouse gasses emitted (Taylor et al. 2012). These classifications include RCP 2.6, which gives a mean increase in global temperature of 1.0°C by the end of the 21st century, RCP 4.5, which projects a mean increase of 1.8°C, RCP 6.0, which projects 2.2°C, and RCP 8.5, which projects 3.7°C. These projections are relative to pre-industrial levels. In this study, RCP 4.5, a stabilisation scenario, is used in comparison to RCP 8.5, a scenario characterised by an increase in greenhouse gases or, as Ongoma et al. (2018c) refer to it, a business as usual scenario, as it is based on the exclusion of mitigating measures.

While it is understood that climate change is a global phenomenon (Byg & Salick 2009), its impacts are mainly felt at the local scale. For policy and decision makers to analyse the impacts of climate change and plan for the future, local and country level projections of meteorological and climatological parameters are necessary. For this reason, many countries are currently involved in the formulation of national climate change adaptation strategies (Greiving & Fleischhauer 2012, RoZ 2016, Republic of South Africa 2017). Robust country-specific climate information is indispensable for this. The goal of this paper, therefore, is to focus on Zambia and examine patterns of extreme precipitation for the period 2021–2100. To this end, the following outline has been used: a brief background of the climate of Zam-

bia is given in Section 2.1, Section 2.2 outlines the data (and sources) used to carry out this work, Section 2.3 describes the methods employed, results and discussion are given in Section 3 and the paper closes with a summary of the findings.

2. METHODS

2.1. The climate of Zambia

Using the Köppen-Geiger climate classification system, Zambia (Fig. 1) is identified as humid subtropical (Geiger 1954), experiencing average temperatures of 28°C in the summer and 5°C in the winter (Hachigonta & Reason 2006, Libanda et al. 2015b). Although much of the land mass is on a plateau (about 1200 m), the intra- and inter-annual distribution of rainfall differs markedly in time and space, with more wetness in the northern half of the country (averaging 1200 mm), decreasing southwards (averaging 800 mm; Libanda et al. 2017a). Large scale circulation mechanisms like the El Niño Southern Oscillation have been linked to rainfall variability over Zambia, with El Niño (La Niña) exerting drier (wetter) than normal conditions over much of the country. Hachigonta et al. (2008) attributed the onset and offset of the rainy season to the fluctuations of the Intertropical Convergence Zone (ITCZ). This was also highlighted in a recent study by Libanda et al. (2017b). The rainy season generally begins in October/November and ceases in March/April.

2.2. Data

Precipitation data from 30 meteorological and climatological stations were obtained from the archives of the Zambia Meteorological Department. These 30 stations were picked based on data availability at the time of analysis. Fig. 1 shows the positions of these stations. The observation data covers the period 1980–2000, which is not long enough to be used to examine the behaviour of models during the baseline period (1961–1990). For this reason, monthly Global Precipitation Climatology Centre (GPCC) rainfall data and Climate Research Unit (CRU) monthly rainfall data were investigated for their ability to capture rainfall data with the aim of using the best dataset to examine the performance of models. Both GPCC (Schneider et al. 2016) and CRU TS3.23 (Harris et al. 2014) are gridded at a spatial resolution of 0.5° × 0.5° and are freely available in netCDF format.

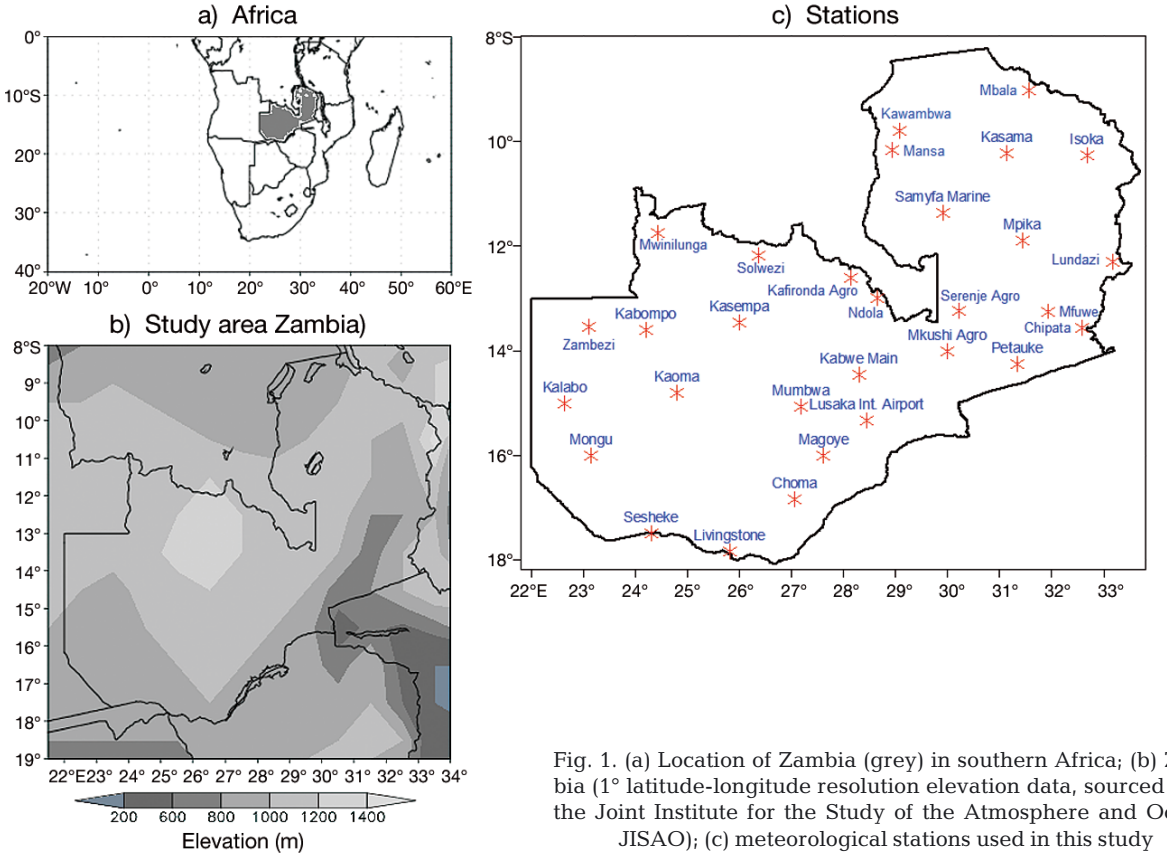

Fig. 1. (a) Location of Zambia (grey) in southern Africa; (b) Zambia (1° latitude-longitude resolution elevation data, sourced from the Joint Institute for the Study of the Atmosphere and Ocean, JISAO); (c) meteorological stations used in this study

The indices are based on data provided by the Canadian Centre for Climate Modelling and Analysis (www.cccma.ec.gc.ca); they cover the period 2021–2100. This study employs 5 of the recommended IPCC and WGCM models from the Coupled Model Intercomparison Project Phase 5 (CMIP5). These models are (1) CNRM-CM5 developed by Météo-France/CNRS, (2) CanESM2 of the Canadian Centre for Climate Modelling and Analysis, (3) EC-Earth, a product of the Royal Netherlands Meteorological Institute, (4) MPI-ESM-LR of the Max Planck Institute for Meteorology and (5) MPI-ESM-MR, also from the Max Planck Institute for Meteorology. These models were chosen from a pool of 20 CMIP5 models (Table 1) based on their skill to reproduce GPCC rainfall patterns over Zambia. A detailed description of the approach used is provided in Section 2.3. Many scientists (e.g. Sillmann et al. 2013b, Ongoma et al. 2018a) have recommended the use of ensembles as opposed to single models because generally, many models agree on the trend but not magnitude of precipitation (Libanda et al. 2017a). Therefore, taking the mean of a group of models gives better results than using single models.

2.3. Methodology

To pick the 5 models included in the ensemble, percent bias (PBias; Gupta et al. 1999) was used to analyse how well the models replicate GPCC data over Zambia. PBias showed the positive or negative behaviour of models relative to GPCC. PBias is a convenient approach because it returns the behaviour of models in percentage. It is widely used in modelling studies; for example, Ongoma et al. (2018b) successfully used PBias to examine how well models simulated precipitation over equatorial east Africa in the 20th century. Standard deviation was also deployed to check the chosen models relative to the GPCC dataset. A Taylor diagram, as proposed by Taylor (2001), was further used to analyse how closely GPCC and CRU are associated with observations.

The models included in the ensemble are of varying resolutions. Therefore, the outputs were regridded to a common resolution using nearest neighbour interpolation before any statistical analyses were done. This reduced the influence exerted by resolution during comparative analyses. This method computes the nearest neighbouring pixel and takes the respective intensity value (Hsing 1999).

Table 2 shows the indices used to classify projections of extreme precipitation over Zambia. Based on the data provided by the Canadian Centre for Climate Modelling and Analysis, the classifications contained herein are what Ongoma et al. (2018c) termed moderate extremes; therefore, *R*25 mm has not been included. In a paper summarising the CLIVAR/GCOS/WMO workshop on indices and indicators for climate extremes, Karl et al. (1999) describes these indices in detail. Many authors (e.g. Klein Tank et al. 2009, Zhang et al. 2011) have also provided detailed

Table 1. Models used in this study

Model name	Modelling Institution	Lat. × Long.
BCC-CSM1-1-M	Beijing Climate Centre, China Meteorological Administration, China	2.8° × 2.8°
BNU-ESM	College of Global Change and Earth System Science, Beijing Normal University	2.8° × 2.8°
CanESM2	Canadian Centre for Climate Modeling and Analysis, Victoria, Canada	2.8° × 2.8°
CCSM4	National Centre for Atmospheric Research, USA	~0.9° × 1.3°
CNRM-CM5	Centre National de Recherches Météorologique, France	~1.4° × 1.4°
CSIRO-MK3.6.0	Commonwealth Scientific and Industrial Research Organization, Australia	~1.875° × 1.875°
EC-Earth	Royal Netherlands Meteorological Institute, Netherlands	1.125° × 1.125°
GFDL-CM3	Geophysical Fluid Dynamics Laboratory, USA	2.5° × ~2.0°
GFDL-ESM2G	Geophysical Fluid Dynamics Laboratory, USA	2.5° × ~2.0°
GFDL-ESM2M	Geophysical Fluid Dynamics Laboratory, USA	2.5° × ~2.0°
GISS-E2-H	NASA Goddard Institute for Space Studies, USA	2° × ~2.5°
HadGEM2-ES	Met Office Hadley Centre, UK	1.875° × 1.275°
IPSL-CM5A-LR	Institut Pierre Simon Laplace, France	3.75° × 1.8°
IPSL-CM5A-MR	Institut Pierre Simon Laplace, France	2.5° × 1.25°
MIROC5	Atmosphere and Ocean Research Institute, The University of Tokyo, Japan	1.4° × 1.4°
MIROC-ESM	Japan Agency for Marine-Earth Science and Technology, Japan	2.8° × 2.8°
MPI-ESM-LR	Max Planck Institute for Meteorology, Germany	1.875° × 1.875°
MPI-ESM-MR	Max Planck Institute for Meteorology, Germany	1.875° × 1.875°
MRI-CGCM3	Meteorological Research Institute, Japan	1.125° × 1.125°
NOR-ESM1-ME	Norwegian Climate Centre	2.5° × 1.8°

Table 2. Indices used in this study. PRCP: precipitation; RR_{ij}: daily precipitation amount on day i in period j; w: daily precipitation amount on a wet day when $RR \geq 1$mm. W represents the number of all wet days in the period under study

Indices	Descriptor	Index calculation	Definition	Unit
Frequency index				
R1 mm	Number of rainfall days	$RR_{ij} \geq 1$ mm	Annual count of days with at least 1 mm of precipitation.	d
R10 mm	Number of heavy rainfall days	$RR_{ij} \geq 10$ mm	Annual count of days when rainfall ≥10 mm.	d
R20 mm	Number of very heavy rainfall days	$RR_{ij} \geq 20$ mm	Annual count of days when rainfall ≥20 mm.	d
CWD	Consecutive wet days	$RR_{ij} \geq 1$ mm	Maximum number of consecutive days with at least 1 mm of precipitation.	d
CDD	Consecutive dry days	$RR_{ij} \leq 1$ mm	Maximum number of consecutive days with less than 1 mm of precipitation.	d
Intensity index				
Rx1day	Daily maximum rainfall	$Rx1day_j = \max(RR_{ij})$	Monthly maximum 1 d rainfall.	mm
Rx5day	5 d maximum rainfall	$Rx5day_j = \max(RR_{ij})$	Monthly maximum 5 d rainfall.	mm
PRCPTOT	Annual wet-day rainfall total	$PRCPTOTj = \sum_{i=1}^{I} RRij$	Annual total rainfall in wet days ($RR > 1$ mm).	mm
SDII	Simple daily intensity index	$SDII_j = \frac{\sum_{w=1}^{W} RR_j}{W}$	Annual mean rainfall when PRCP ≥ 1 mm.	mm d^{-1}
R95p	Very wet day	$R95p_j = \sum_{W=1}^{W} RR_{wj}$	Annual total rainfall when $RR >$ 95th percentile.	mm
R99p	Extremely wet day	$R99p_j = \sum_{W=1}^{W} RR_{wj}$	Annual total rainfall when $RR >$ 99th percentile.	mm

descriptions of these indices. Further documentation is available from the World Research Climate Programme at www.wcrp-climate.org/data-etccdi.

The design of the analysis described here refers to a 1961–1990 baseline. Many researchers, including Tomozeiu et al. (2014) and Ongoma et al. (2018c), have utilised this baseline in climate change studies around the world. Projections were divided into 2 separate 30 yr periods, i.e. 2021–2050 and 2071–2100; precipitation extremes were studied during these periods relative to the 1961–1990 baseline.

The Mann-Kendall test (Mann 1945, Kendall 1975) was used to identify trends in the projected precipitation. While other methods of characterising trends exist, the Mann-Kendall test has been heralded by many scientists as the most robust methodology for trend characterisation. For instance, Ongoma et al. (2018d) used it to characterise trends of extreme weather events over equatorial East Africa, focussing on Uganda and Kenya. Adamowski & Bougadis (2003) also used it alongside the L-moments method to detect trends in extreme rainfall in Canada. In general, the Mann-Kendall test is given as:

$$s = \sum_{i=1}^{n-1} \sum_{j=i+1}^{n} sig(x_i - x_j) \quad (1)$$

In this case, n is the sample size, and x_i and x_j are sequential values of x. The p-value, after the Z-test, was used in comparison to the $\alpha = 5\%$ confidence level; if the p-value is lower (higher) than α then it is taken to be significant (insignificant). The null hypothesis (H_0) states that there is no trend in the series and the alternative (H_1) that there is a trend in the series. Mathematically, the variance (VAR) of S is given as:

$$VAR(S) = \frac{1}{18}[n(n-1)(2n+5) - \sum_{p-1}^{g} t_p(t_p-1)(2t_p+5)] \quad (2)$$

where g is the number of tied groups, n is the number of data points and t_p is the number of observations in the pth group.

To quantify the magnitude of the trends, Sen's slope estimator was used (Sen 1968). Like the Mann-Kendall test, Sen's slope estimator uses a non-parametric approach and it is given as:

$$Q = \frac{Y_{i'} - Y_i}{i' - i} \quad (3)$$

where Q is a slope estimate, $Y_{i'}$ and Y_i are the values at times i' and i, where i' is greater than i. Examples of studies that have used Sen's slope include those of Gocic & Tajkovic (2013) in Serbia, and Sanogo et al.

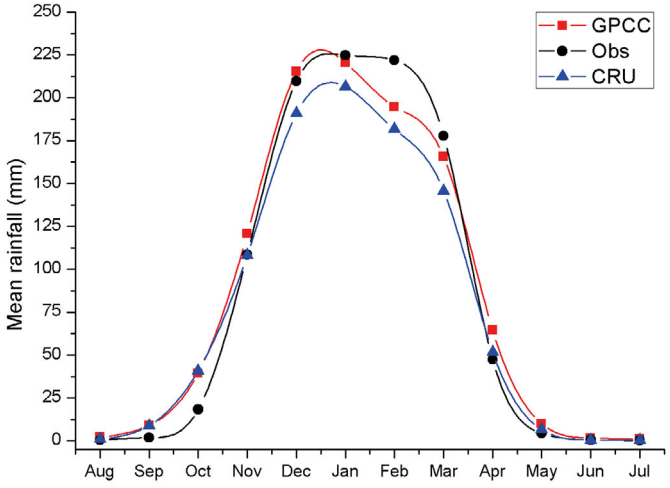

Fig. 2. Mean annual cycle of precipitation (mm) over Zambia based on observations (black), and the GPCC (red) and CRU (blue) datasets, averaged over longitudes 21.8° to 34° E and latitudes 18° to 8° S for the period 1980–2000

(2015), who studied spatio-temporal characteristics of rainfall recovery in West Africa.

The Probability Distribution Function (PDF) is useful for characterising the relative frequency of occurrence of given values within a dataset under consideration (Wilks 1995, Fallmann et al. 2017). Here, changes in the temporal intensity of precipitation in Zambia are described using PDFs. Empirical distribution was employed to generate the PDFs for the 3 periods, i.e. historical/baseline (1961–1990), 2021–2050 and 2071–2100. To understand the statistical significance of the changes in the PDFs, a 2-tailed Kolmogorov-Smirnov test was used (Jupp et al. 2010).

3. RESULTS AND DISCUSSION

3.1. Model performance

Fig. 2 shows the comparison of the mean annual cycles from the GPCC and CRU datasets and observations. Results indicate that both the GPCC and CRU datasets were able to reproduce observations of rainfall received from October/November to March/April. All the datasets produced a distinct dry season from May to September, as has been observed by others (e.g. Hachigonta & Reason 2006, Libanda et al. 2015b).

The ability of the GPCC and CRU datasets to mimic rain gauge data in reproducing interannual variability in precipitation is presented in Fig. 3. Although the magnitude of annual changes in the reanalysed datasets does not precisely match the observations, these results indicate that all the datasets were able to accurately capture the trend of reducing precipitation across Zambia.

The overall aim of comparing the GPCC and CRU data to observations was to find a suitable dataset for examining the skill of models for the baseline period (1961–1990). The observation data, which covers the period 1980–2000, was not long enough for this purpose. The results presented in Figs. 2 & 3 show that both datasets adequately capture rain gauge data. The GPCC dataset was subsequently used, based on the results presented in Fig. 4. From these results (Taylor diagram), it can be seen that both the GPCC and CRU datasets are strongly correlated with the observations, with the GPCC set showing a slightly stronger correlation (0.83 for GPCC and 0.80 for CRU). The GPCC dataset generally performs well over Africa. This is mirrored in the work of Nicholson et al. (2003), who compared the performance of GPCC data to a network of 515 observatory stations and found good agreement. Having validated that GPCC data agrees with observed data, this was used in subsequent analyses in this study.

While many scientists (e.g. Sillmann et al. 2013b, Ongoma et al. 2018a) have recommended the use of ensembles as opposed to single models, it is also well documented that ensembles containing models with poor skill over a region of study can lower the overall performance of the ensemble (Fotso-Nguemo et al. 2018). This is because model performance varies

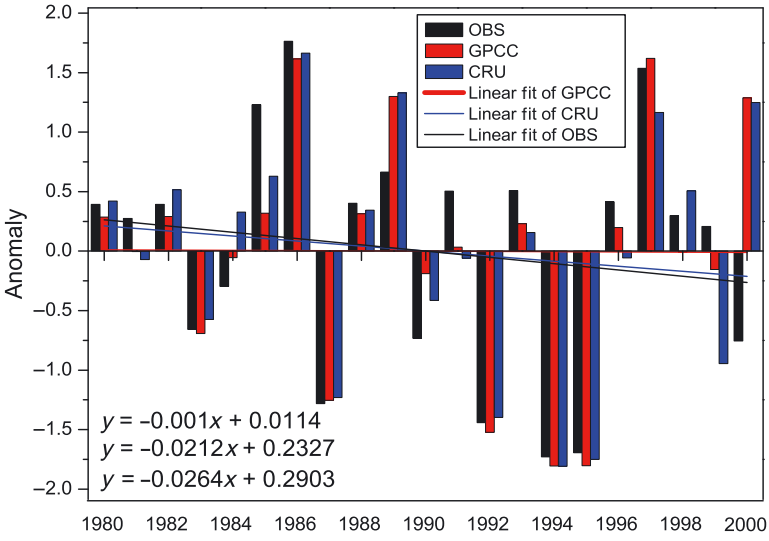

Fig. 3. Standardised rainfall anomaly across Zambia based on observations (black), GPCC (red) and CRU (blue), averaged over longitudes 21.8° to 34° E and latitudes 18° to 8° S for the period 1980–2000. The equations are for GPCC, CRU and observations, respectively

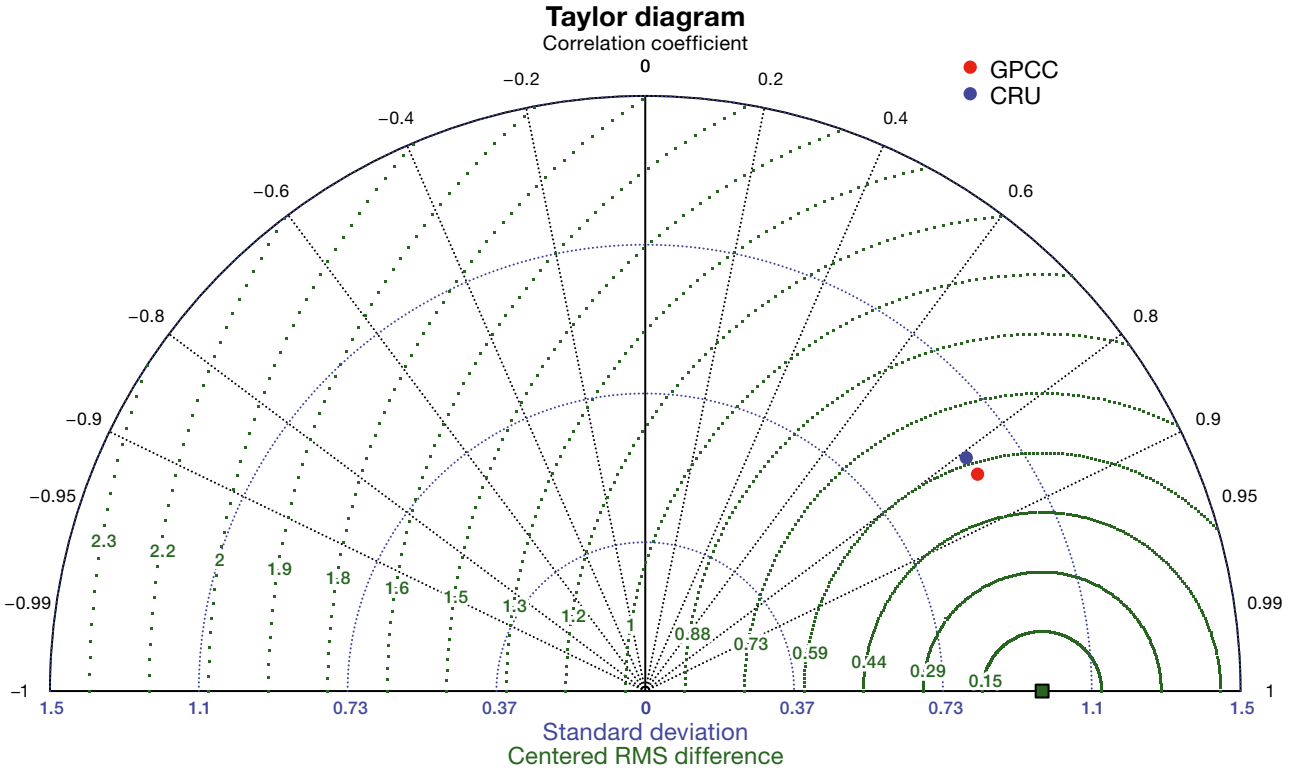

Fig. 4. Taylor diagram of GPCC and CRU data against observations for the period 1980–2000, averaged over longitudes 21.5° to 34° E and latitudes 18° to 8° S

from one region to another. In this study, the performance of 20 models (Table 1) over Zambia was examined. Results (Fig. 5a) show that only 5 models performed within ±5% PBias of GPCC. These models were CNRM-CM5, CanESM2, EC-Earth, MPI-ESM-LR and MPI-ESM-MR. The resulting ensemble had a 1.1% PBias and was better than any of the individual models. However, it is worth noting that users of this ensemble should apply caution as it still overestimates GPCC data.

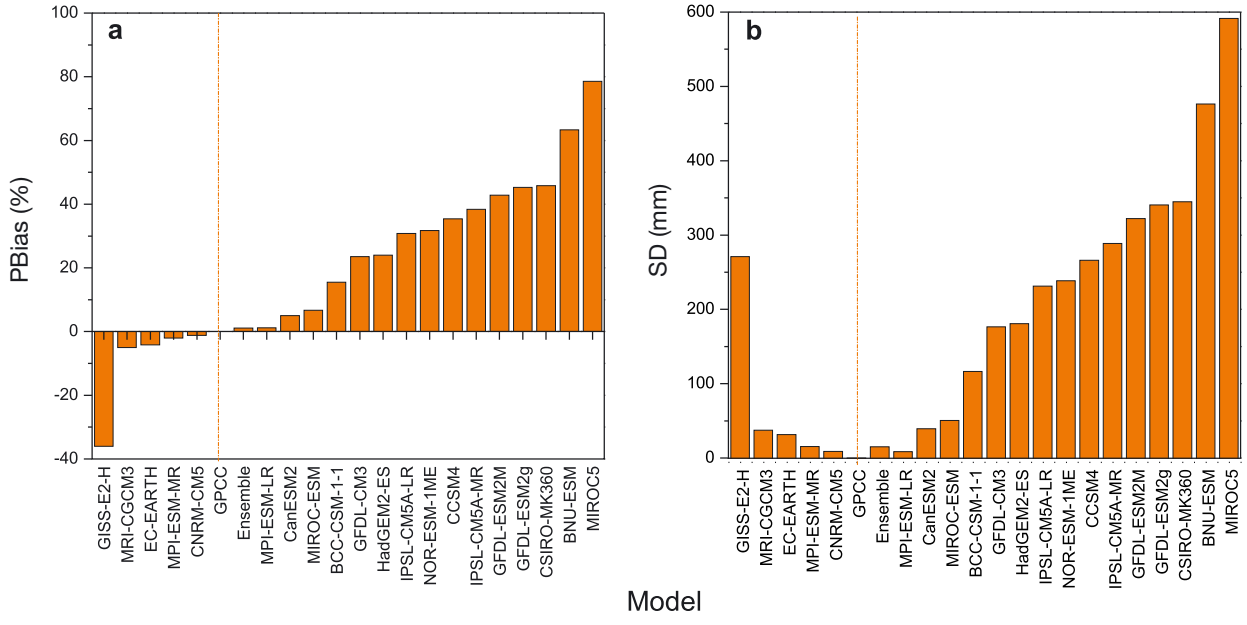

Fig. 5. (a) Area-averaged annual PBias of rainfall; (b) standard deviation relative to GPCC data for each GCM for the period 1961–1990 over Zambia. Dotted line: GPCC

Results further indicate (Fig. 5a) that apart from GISS-E2-H, MRI-CGCM3, EC-Earth, MPI-ESM-MR and CNRM-CM5, all the models showed positive bias relative to GPCC and this contributed to the resultant positive bias of the ensemble. With a PBias of −36% (78.6%), GISS-E2-H (MIROC5) was the highest negatively (positively) biased model. Standard deviation (Fig. 5b) was used to further examine how well GPCC data mimics observations. These results indicate a similar pattern to that observed in the PBias computation. In general, lower deviation was observed in the 5 ensemble models compared to the other 15. Overall, the highest (lowest) departure from GPCC was observed in MIROC5 (MPI-ESM-LR) with a standard deviation of 591.3 mm (8.6 mm).

Table 3 gives a statistical summary of the performance of each model. Of the 20 models, 12 exhibited a negative correlation. Although the remaining 8 models were positively correlated, the correlation coefficients only ranged between 0.01 and 0.32, indicating weak agreement between the models and GPCC data over Zambia. Similar findings were noted by Ongoma et al. (2018b) in their study over East Africa.

Table 3. Statistical association between models and GPCC data over Zambia

Model	Annual mean	Correlation coefficient	RMSE
BCC-CSM-1-1	1228.32	0.07	224.01
BNU-ESM	1737.37	−0.10	693.69
CanESM2	1119.21	−0.10	163.60
CCSM4	1439.82	0.01	407.72
CNRM-CM5	1051.05	−0.27	144.89
CSIRO-MK3.6.0	1551.39	−0.18	519.97
EC-Earth	1019.01	−0.06	142.13
Ensemble	1042.29	−0.19	128.58
GFDL-CM3	1313.36	−0.07	295.70
GFDL-ESM2G	1545.35	−0.08	504.00
GFDL-ESM2M	1519.51	−0.24	483.65
GISS-E2-H	680.51	−0.02	415.07
GPCC	1063.76	1.00	0.00
HadGEM2-ES	1319.31	0.12	295.94
IPSL-CM5A-LR	1391.02	0.32	361.07
IPSL-CM5A-MR	1472.16	0.19	433.03
MIROC5	1900.10	−0.02	852.25
MIROC-ESM	1135.01	0.00	202.05
MPI-ESM-LR	1076.02	0.02	131.48
MPI-ESM-MR	1042.08	−0.11	137.55
MRI-CGCM3	1010.75	0.23	135.95
NOR-ESM1-ME	1401.25	0.18	379.74

3.2. Temporal and spatial variability of rainfall frequency

The frequency of extreme precipitation was studied and characterised using indices shown in Table 2. Generally, a significant increase in the number of consecutive dry days (CDD) (Fig. 6a) was projected over Zambia, especially beginning from the year 2050 and continuing to the end of the century. An increase in the number of CDD will negatively impact the agricultural sector because this is strongly correlated with critically reduced soil moisture (Hottenstein et al. 2015). These climate patterns will be key for strategic planning to ensure food security. Agriculture is not the only sector that is challenged by CDD; a study by Chen et al. (2014) on the influence of CDD on burned areas in southwestern China found that CDD predominantly boosted large fires affecting areas of up to 100 ha or more. Such large fires are usually catastrophic, causing significant socio-economic disruptions and threatening ecosystem provisioning. Under RCP 4.5, Sen's slope for CDD is 0.323 but steepens to 0.439 under RCP 8.5. In both cases, the risk of rejecting the null hypothesis

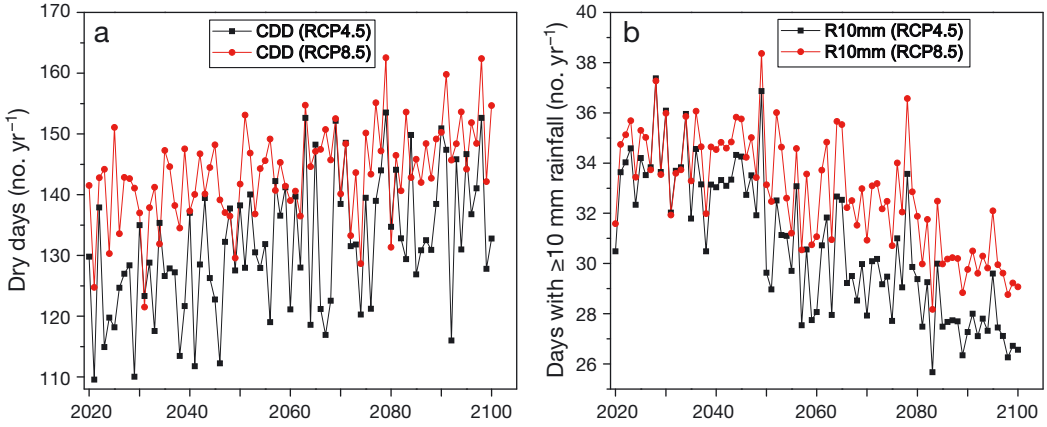

Fig. 6. Timeseries of (a) consecutive dry days (CDD) and (b) number of days with at least 10 mm precipitation (*R*10 mm). Baseline period for anomalies calculation is 1961–1990

H_0 when it is true is lower than 0.01 %. In contrast to CDD, consecutive wet days (CWD) are projected to decrease over Zambia.

Fig. 6b shows the temporal distribution of days when rainfall is ≥10 mm. These results indicate a reduction in the trend with slopes of −0.5 (RCP 4.5) and −0.6 (RCP 8.5). It is important to note that $R10$ mm and $R1$ mm both refer to the number of days; therefore, when the number of days receiving extreme precipitation reduces, the intensity increases, as shown in Section 3.3.

Spatially, the intensification of CDD under RCP 4.5 is observed only over Eastern, Lusaka and parts of Southern Province for the period 2021–2050 (Fig. 7a). Towards the end of the century (Fig. 7b), more areas, including parts of Northern and Central Province, become affected. This will have a negative impact on the Mkushi farming block, one of the country's major producers of Zambia's staple food (maize). Under RCP 8.5 (Fig. 7c,d), CDD intensifies further to cover the whole of Southern, Central and Western Province and extending to Luapula Province towards the end of the century. Taken together, these results (Fig. 7) show that the spatial intensification of CDDs will exhibit a north to southeast pattern, i.e. the northern half, especially over the boundary between Congo and Zambia, will have less reduction (more rainfall) than the southeastern part. Eastern Province will be more affected than Southern. Therefore, the downward trend of

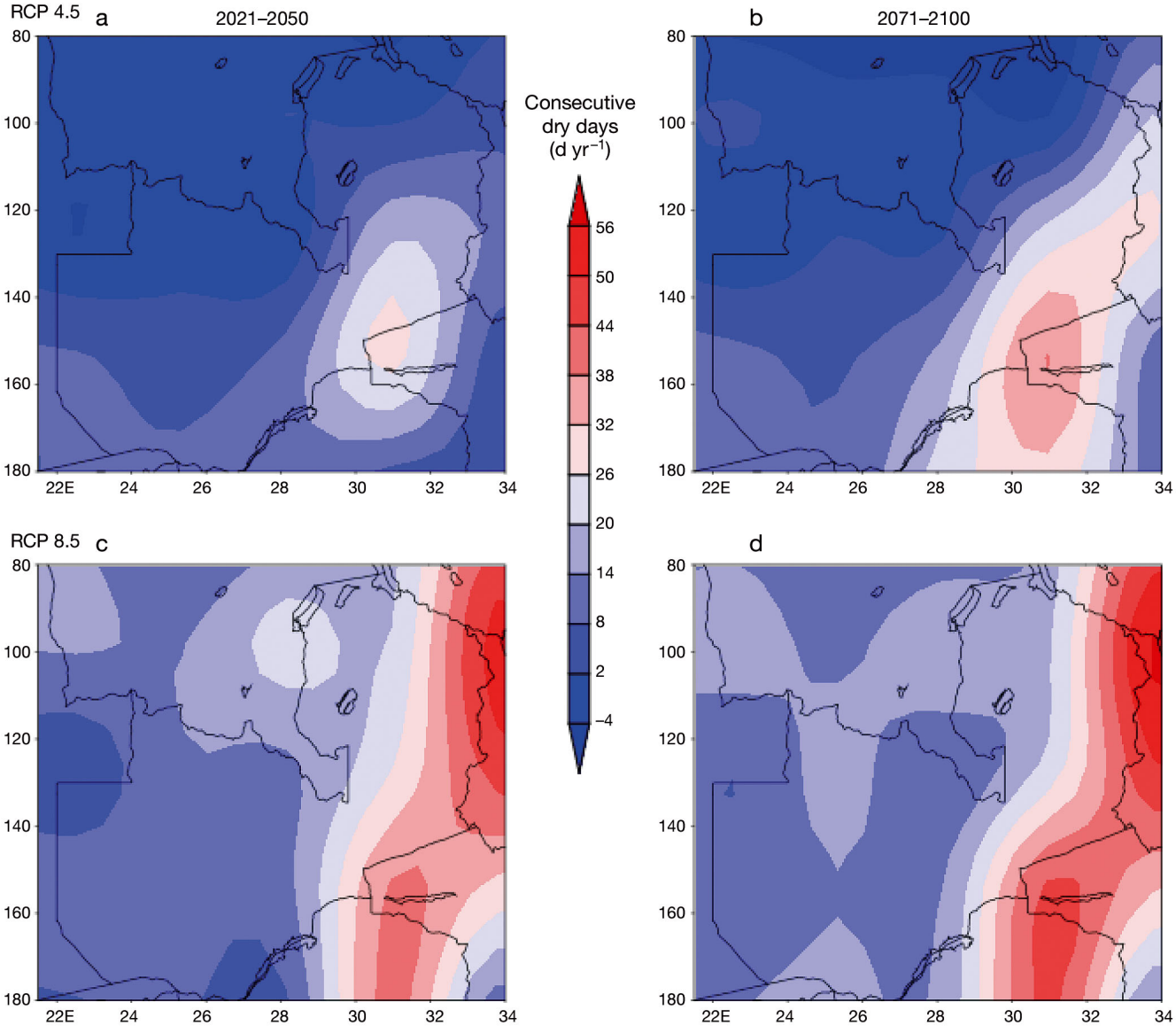

Fig. 7. Anomalies of consecutive dry days (CDD). (a,b) RCP 4.5 and (c,d) RCP 8.5 simulations relative to the 1961–1990 reference period

Table 4. Statistical summary of precipitation frequency over Zambia for the period 2020–2100 computed in respect to α = 0.05. Significant results are given in **bold**. See Table 2 for definition of variables

Variable	RCP	Sen's slope	Risk of rejecting H_0 when true (%)
*R*1 mm	4.5	−0.225	**0.01**
*R*1 mm	8.5	−0.275	**0.01**
*R*10 mm	4.5	−0.525	2.22
*R*10 mm	8.5	−0.631	3.99
*R*20 mm	4.5	−0.018	38.22
*R*20 mm	8.5	−0.028	5.42
CWD	4.5	−0.074	6.24
CWD	8.5	−0.082	23.43
CDD	4.5	0.323	**0.03**
CDD	8.5	0.439	**0.04**

precipitation from the north to the south of the country that has been observed in previous studies (e.g. Hachigonta et al. 2008, Libanda et al. 2015b) using rain gauge data is projected to continue through the middle to the end of the century. These results are presented as differences between (1) the middle of the century (2021–2050) and the baseline period (1961–1990), and (2) the end of the century (2071–2100) and the baseline period (1961–1990).

A significant downward trend is projected in the frequency of days with at least 1 mm of precipitation. On Sen's slope estimator, this downward trend is graded as −0.225 under RCP 4.5 and −0.275 under RCP 8.5. Under both concentration pathways (RCP 4.5 and RCP 8.5), the risk of rejecting the null hypothesis H_0 when it is true is lower than 0.01%. A summary of the frequency results is given in Table 4.

3.3. Temporal and spatial variability of precipitation intensity

Annual total rainfall in wet days (daily precipitation > 1 mm) exhibits a declining trend (Fig. 8a,b). The variance decreases significantly, especially during the 2071–2100 period; the tails of the PDFs extend towards lower precipitation amounts during this period. These findings are in agreement with those of Shongwe et al. (2011), who projected a decline in annual precipitation over the broader southern African region.

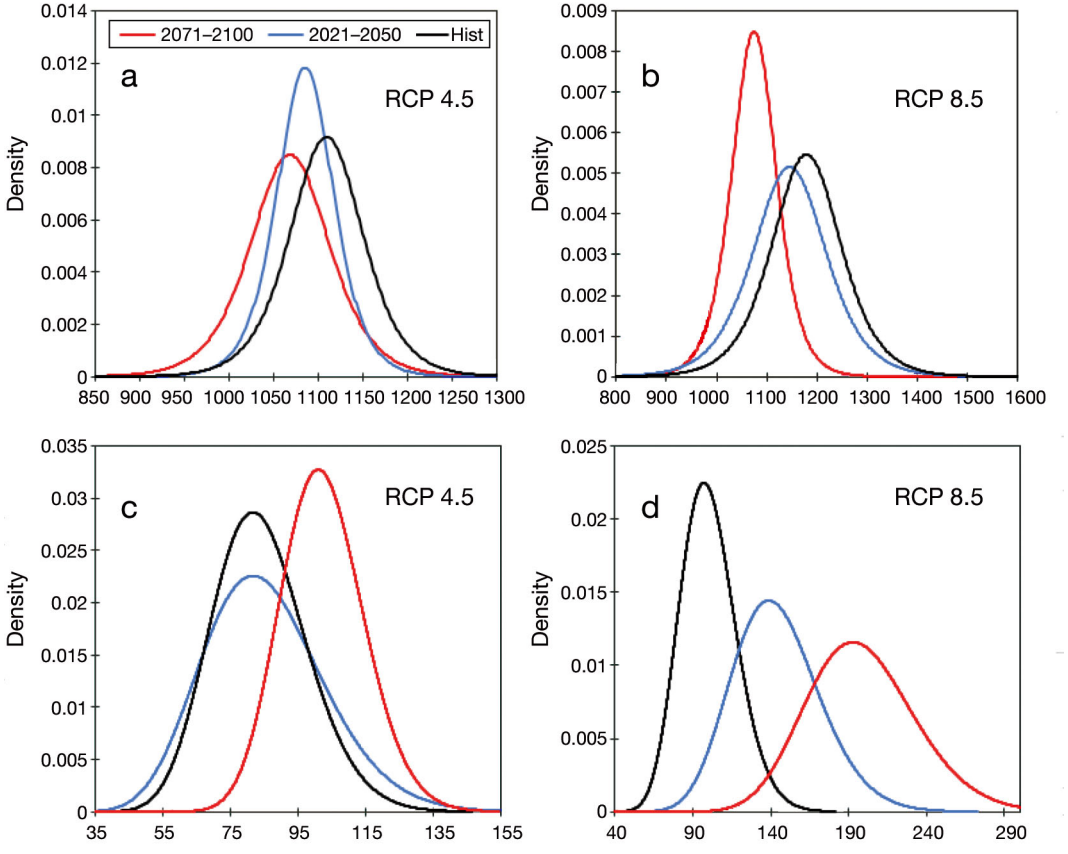

Fig. 8. Probability density functions of (a,b) annual total rainfall in wet days (mm yr^{-1}) and (c,d) extremely wet days (mm yr^{-1}) relative to the 1961–1990 reference period. (a,c) RCP 4.5 and (b,d) RCP 8.5 simulations

Overall, while the frequency of precipitation is predicted to reduce over the country, the intensity exhibits an upward trend. For instance, the wettest day of the season (Fig. 8), i.e. the 99th percentile of daily maximum precipitation in any given season, is projected to increase with a Sen's slope of 0.424 under RCP 4.5 and 0.479 under RCP 8.5. Although significant change in rainfall variance at the 5% significance level is observed in both *R*99p and PRCPTOT, the negative shifts of PDFs observed in PRCPTOT (Fig. 8a,b) are reversed here. These heavy rainfalls will result in flooding that poses risk to properties and lives because changes in variance exert greater influence on extremes than mean rainfall changes (Katz & Brown 1992). Many studies have shown that when daily accumulated total precipitation exceeds the 90th, 95th or 99th percentiles of the rainfall climatology of the area of study, this results in pluvial and fluvial floods that cause damage and significant losses. For instance, Christensen & Christensen (2003) found that precipitation that exceeded the 95th percentile over continental Europe resulted in catastrophic flooding. In Fig. 8c,d, results are presented as PDFs and both RCP 4.5 and 8.5 projections exhibit a shift towards more intense precipitation commensurate to an increase in radiative forcing over time.

With an increase in radiative forcing, extremely heavy precipitation (*R*99p) is projected to intensify in the central parts of the country stretching from Northern and Luapula Province, especially under RCP 8.5 (Fig. 9c,d). The Northern and Luapula regions are home to some of Zambia's major water bod-

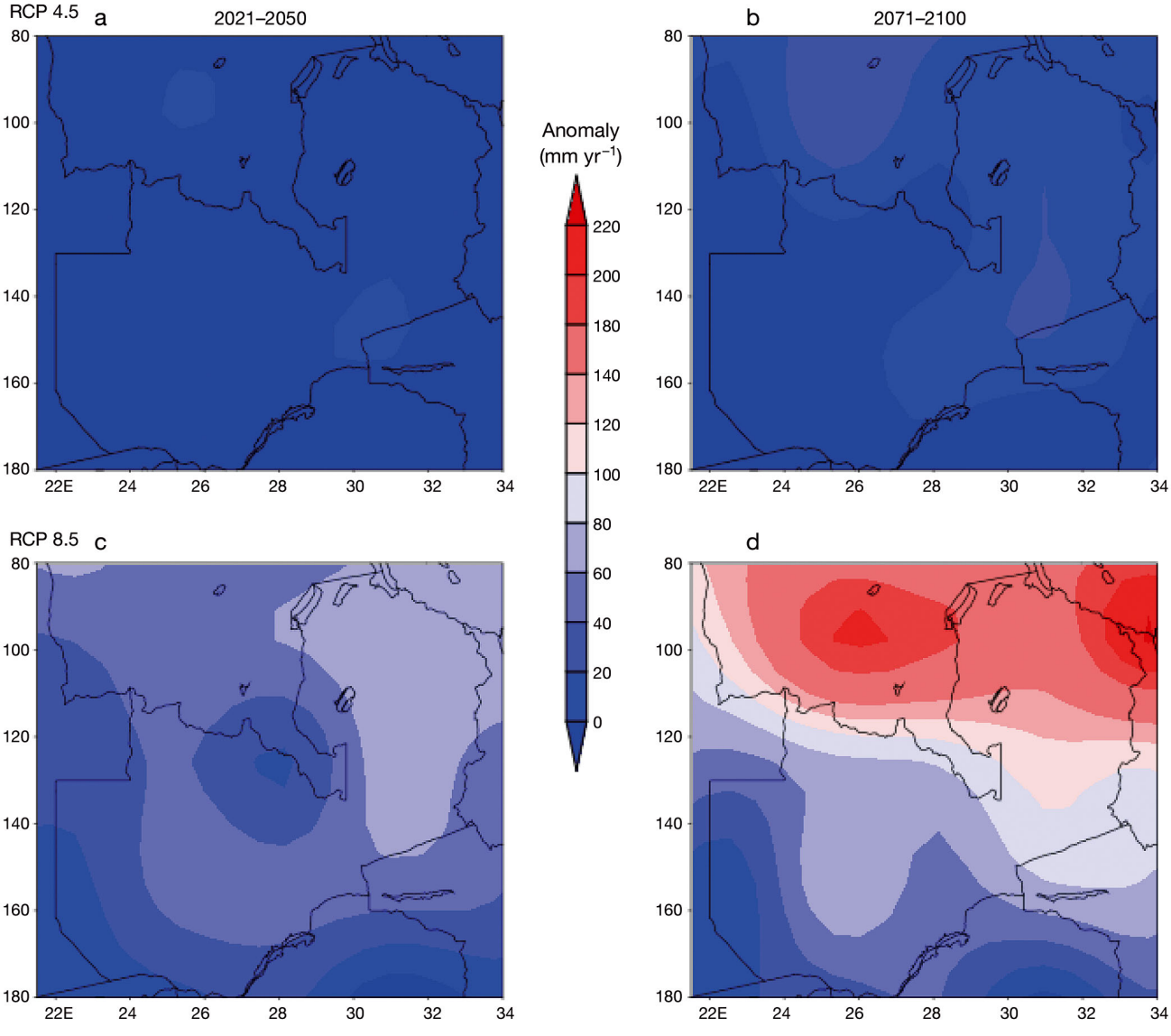

Fig. 9. Anomalies of *R*99p (a,b) RCP 4.5 and (c,d) RCP 8.5 simulations relative to the 1961–1990 reference period

ies, e.g. Lake Bangweulu, Mweru and Mweru Wantipa (Libanda et al. 2018). With intensified precipitation, adaptive strategies against flooding around this area will be of major importance. Inundation of floodwater into homes, displacement of people, mudslides and erosion of stream banks and lakeshores are common in the wake of intensified precipitation (Shongwe et al. 2011). Fig. 9 shows the spatial patterns of *R*99p. Again, these results are presented as differences between (1) the middle of the century (2021–2050) and the baseline period (1961–1990), and (2) the end of the century (2071–2100) and the baseline period (1961–1990).

Trends of precipitation intensity, both significant and insignificant, are summarised in Table 5. These conclusions are consistent with the findings of Pinto et al. (2016) who used CORDEX models to project extreme precipitations over the whole southern African region. Although they used a different reference period (1976–2005), they showed conclusively that annual total precipitation will decrease, CDD will increase and *R*95p will increase towards the end of the 21st century.

4. CONCLUSION AND SUMMARY

Climate change is a global phenomenon, but its impacts are mainly felt at the local scale. This necessitates research that contributes meaningful understanding of future climate variations at the local or country level. This study investigated future (2021–2100) trends of extreme precipitation over Zambia using ETCCDI indices. Broadly, an increase (decline) in precipitation intensity (frequency) is predicted.

Table 5. Statistical summary of precipitation intensity over Zambia for the period 2020–2100 computed in respect to $\alpha = 0.05$. Significant results are given in **bold**. See Table 2 for definition of variables

Variable	RCP	Sen's slope	Risk of rejecting H_0 when true (%)
*R*x1day	4.5	0.035	**0.01**
*R*x1day	8.5	0.092	**0.01**
*R*x5day	4.5	0.329	**0.01**
*R*x5day	8.5	0.429	**0.01**
PRCPTOT	4.5	−0.035	0.63
PRCPTOT	8.5	−0.15	**0.04**
SDII	4.5	0.293	**0.01**
SDII	8.5	0.394	**0.03**
*R*95p	4.5	0.388	**0.01**
*R*95p	8.5	0.419	**0.01**
*R*99p	4.5	0.424	**0.02**
*R*99p	8.5	0.479	**<0.01**

Specifically, a significant increase in the number of CDD is projected over Zambia, especially beginning from the year 2050 to the end of the century. An increase in the number of CDD will negatively impact the agricultural sector, ecosystem services and water resources management. Under RCP 4.5, Sen's slope for CDD is 0.323, but steepens to 0.439 under RCP 8.5. In both cases, the risk of rejecting the null hypothesis H_0 when it is true is lower than 0.05%. In contrast to CDD, CWD are projected to decrease over Zambia. A significant downward trend is projected for the frequency of days with at least 10 mm of precipitation. This decrease is apparent beginning from around 2040 up to the end of the century. Sen's slope for this downward trend is graded as −0.525 under RCP 4.5 and −0.631 under RCP 8.5. In similar pattern to *R*10 mm, *R*1 mm is observed to decline under RCP 8.5 with a Sen's slope of −0.275. Spatially, the intensification of CDD under RCP 4.5 is observed only over Eastern, Lusaka and parts of Southern Province, but under RCP 8.5, the number of CDD intensifies further to cover the whole of Southern, Central and Western Province.

The wettest day of the season, i.e. the 99th percentile of daily maximum precipitation in any given season, is projected to increase with a Sen's slope of 0.424 under RCP 4.5 and 0.479 under RCP 8.5. These heavy rainfalls will result in flooding, posing risk to properties and lives.

The results described here give an overview of the expected trends in Zambia. These results can act as guidelines for strategic planning for flood and drought prevention. This work also forms a baseline for future, more robust, climate research in Zambia.

Acknowledgements. B.L. carried out this work while on a PhD scholarship sponsored by the University of Edinburgh; the University is hereby acknowledged for financial support and for creating an environment which nurtures research activities. The editor and the 2 anonymous reviewers are acknowledged for their invaluable feedback. The Zambia Meteorological Department (ZMD), the Canadian Centre for Climate Modelling and Analysis (CCCMA), the Joint Institute for the Study of the Atmosphere and Oceans (JISAO), NCEP/NCAR and the Climate Research Unit of the University of East Anglia are acknowledged for the datasets used in this study.

LITERATURE CITED

ACAPS (2017) ACAPS briefing note: floods, 26 January 2017. https://reliefweb.int/report/mozambique/acaps-briefing-note-floods-26-january-2017 (accessed 25 March 2018)

ACT Alliance (2017) Floods emergency—Malawi. https://reliefweb.int/report/malawi/act-alliance-alert-floods-emergency-malawi (accessed 25 March 2018)

Adamowski K, Bougadis J (2003) Detection of trends in annual extreme rainfall. Hydrol Processes 17:3547–3560

Byg A, Salick J (2009) Local perspectives on a global phenomenon—climate change in Eastern Tibetan villages. Glob Environ Change 19:156–166

Chen F, Fan Z, Niu S, Zheng J (2014) The influence of precipitation and consecutive dry days on burned areas in Yunnan Province, southwestern China. Adv Meteorol 2014:748923

Chinowsky PS, Schweikert AE, Strzepek NL, Strzepek K (2015) Infrastructure and climate change: a study of impacts and adaptations in Malawi, Mozambique, and Zambia. Clim Change 130:49–62

Christensen JH, Christensen OB (2003) Climate modelling: severe summertime flooding in Europe. Nature 421: 805–806

Davis CL (2011) Climate risk and vulnerability: a handbook for Southern Africa. Council for Scientific and Industrial Research, Pretoria

Engelbrecht CJ, Engelbrecht FA, Dyson LL (2013) High-resolution model-projected changes in mid-tropospheric closed-lows and extreme rainfall events over southern Africa. Int J Climatol 33:173–187

Fallmann J, Wagner S, Emeis S (2017) High resolution climate projections to assess the future vulnerability of European urban areas to climatological extreme events. Theor Appl Climatol 127:667–683

Fotso-Nguemo TC, Chamani R, Yepdo ZD, Sonkoué D, Matsaguim CN, Vondou DA, Tanessong RS (2018) Projected trends of extreme rainfall events from CMIP5 models over Central Africa. Atmos Sci Lett 19:e803

Geiger R (1954) Klassifikationen der Klimate nach W. Köppen. In: Landolt-Börnstein: Zahlenwerte und Funktionen aus Physik, Chemie, Astronomie, Geophysik und Technik, alte Serie, Vol 3. Springer, Berlin, p 603–607

Gocic M, Trajkovic S (2013) Analysis of changes in meteorological variables using Mann-Kendall and Sen's slope estimator statistical tests in Serbia. Global Planet Change 100:172–182

Greiving S, Fleischhauer M (2012) National climate change adaptation strategies of European states from a spatial planning and development perspective. Eur Plann Stud 20:27–48

Gupta HV, Sorooshian S, Yapo PO (1999) Status of automatic calibration for hydrologic models: comparison with multilevel expert calibration. J Hydrol Eng 4:135–143

Hachigonta S, Reason CJC (2006) Interannual variability in dry and wet spell characteristics over Zambia. Clim Res 32:49–62

Hachigonta S, Reason C, Tadross M (2008) An analysis of onset date and rainy season duration over Zambia. Theor Appl Climatol 91:229–243

Hansen J, Sato M, Hearty P, Ruedy R and others (2016) Ice melt, sea level rise and superstorms: evidence from paleoclimate data, climate modeling, and modern observations that 2°C global warming could be dangerous. Atmos Chem Phys 16:3761–3812

Harris I, Jones PD, Osborn TJ, Lister DH (2014) Updated high-resolution grids of monthly climatic observations—the CRU TS3.10 dataset. Int J Climatol 34:623–642

Hottenstein JD, Ponce-Campos GE, Moguel-Yanes J, Moran MS (2015) Impact of varying storm intensity and consecutive dry days on grassland soil moisture. J Hydrometeorol 16:106–117

Hsing T (1999) Nearest neighbor inverse regression. Ann Stat 27:697–731

IPCC (2001) Climate change: the scientific basis. Contribution of working group 1 to the third assessment report of the Intergovernmental Panel on Climate Change. Houghton JT, Ding Y, Griggs DJ, Noguer M, and others (eds). Cambridge University Press, Cambridge, and New York, NY

IPCC (2012) Managing the risks of extreme events and disasters to advance climate change adaptation. A special report of working groups I and II of the Intergovernmental Panel on Climate Change. Field CB, Barros V, Stocker TF, Qin D and others (eds). Cambridge University Press, Cambridge, and New York, NY

IPCC (2013) Climate change: the physical science basis. Contribution of working group I to the fifth assessment report of the Intergovernmental Panel on Climate Change. Stocker TF, Qin D, Plattner GK, Tignor M and others (eds). Cambridge University Press, Cambridge, and New York, NY

IPCC (2014) Climate change: synthesis report. Contribution of working groups I, II and III to the fifth assessment report of the Intergovernmental Panel on Climate Change. Core Writing Team, Pachauri RK, Meyer LA (eds). IPCC, Geneva

Jupp TE, Cox PM, Rammig A, Thonicke K, Lucht W, Cramer W (2010) Development of probability density functions for future South American rainfall. New Phytol 187:682–693

Kaplan D (2009) Structural equation modeling. Sage Publications, Los Angeles

Karl TR, Nicholls N, Ghazi A (1999) CLIVAR/ GCOS/WMO workshop on indices and indicators for climate extremes: workshop summary. Clim Change 42:3–7

Katz RW, Brown BG (1992) Extreme events in a changing climate: variability is more important than averages. Clim Change 21:289–302

Kendall MG (1975) Rank correlation methods, 4th edn. Griffin, London

Klein Tank A, Zwiers FW, Zhang X (2009) Guidelines on analysis of extremes in a changing climate in support of informed decisions for adaptation. Climate data and monitoring. WCDMP-No. 72, WMO-TD No. 1500

Libanda B, Ogwang BA, Ongoma V, Chilekana N, Nyasa L (2015a) Diagnosis of the 2010 DJF flood over Zambia. Nat Hazards 81:189–201

Libanda B, Nkolola B, Musonda B (2015b) Rainfall variability over northern Zambia. J Sci Res Rep 6:416–425

Libanda B, David A, Banda N, Wang L, Ngonga C, Linda N (2017a) Predictor selection associated with statistical downscaling of precipitation over Zambia. Asian J Phys Chem Sci 1:AJOPACS.31545

Libanda B, Zheng M, Banda N (2017b) Variability of extreme wet events over Malawi. Geographica Pannonica 21:212–223

Libanda B, Zheng M, Ngonga C (2018) Spatial and temporal patterns of drought in Zambia. J Arid Land (in press)

Lorenz R, Davin EL, Seneviratne SI (2012) Modeling land-climate coupling in Europe: impact of land surface representation on climate variability and extremes. J Geophys Res Atmos 117:D20109

Mann HB (1945) Non-parametric tests against trend. Econometrica 13:245–259

Mason SJ, Joubert AM (1997) Simulated changes in extreme rainfall over southern Africa. Int J Climatol 17:291–301

Nangombe S, Madyiwa S, Wang J (2018) Precursor conditions related to Zimbabwe's summer droughts. Theor Appl Climatol 131:413–431

New M, Hewitson B, Stephenson DB, Tsiga A and others

(2006) Evidence of trends in daily climate extreme climate events over southern and west Africa. J Geophys Res Atmos 111:D14102

Nicholson SE, Some B, McCollum J, Nelkin E and others (2003) Validation of TRMM and other rainfall estimates with a high-density gauge dataset for West Africa. I. Validation of GPCC rainfall product and pre-TRMM satellite and blended products. J Appl Meteorol 42:1337–1354

Ongoma V, Chen H, Gao C (2018a) Projected changes in mean rainfall and temperature over East Africa based on CMIP5 models. Int J Climatol 38:1375–1392

Ongoma V, Chen H, Gao C (2018b) Evaluation of CMIP5 twentieth century rainfall simulation over the equatorial East Africa. Theor Appl Climatol (in press) doi:10.1007/s00704-018-2392-x

Ongoma V, Chen H, Gao C, Nyongesa AM, Polong F (2018c) Future changes in climate extremes over Equatorial East Africa based on CMIP5 multimodel ensemble. Nat Hazards 90:901–920

Ongoma V, Chen H, Omony GW (2018d) Variability of extreme weather events over the equatorial East Africa, a case study of rainfall in Kenya and Uganda. Theor Appl Climatol 131:295–308

Pinto I, Lennard C, Tadross M, Hewitson B and others (2016) Evaluation and projections of extreme precipitation over southern Africa from two CORDEX models. Clim Change 135:655–668

Pohl B, Macron C, Monerie PA (2017) Fewer rainy days and more extreme rainfall by the end of the century in Southern Africa. Sci Rep 7:46466

Reason C (2016) Climate of southern Africa. Oxford research encyclopedia of climate science. Oxford University Press, Oxford, p 1–43

ReliefWeb (2017) Southern Africa: floods – Jan 2017. https://reliefweb.int/disaster/fl-2017-000012-moz (accessed 25 March 2018)

Republic of South Africa (2017) National climate change adaptation strategy Republic of South Africa www.environment.gov.za/sites/default/files/reports/nationalclimate_changeadaptation_strategyforcomment_nccas.pdf (accessed on 24 March 2018)

RoZ (Republic of Zambia) (2008) Zambia's report on the various thematic cluster of issues submitted to the United Nations Commission on Sustainable Development (UNCSD-16) www.un.org/esa/dsd/dsd_aofw_ni/ni_pdfs/NationalReports/zambia/ZambiaCSD16-17_full_report.pdf (accessed on 12 September 2014)

RoZ (Republic of Zambia) (2016) National policy on climate change. Ministry of National Development Planning www.mndp.gov.zm/download/ministry-of-National-Development.-2.pdf (accessed 24 March 2018)

Sanogo S, Fink AH, Omotosho JA, Ba A, Redl R, Ermert V (2015) Spatio-temporal characteristics of the recent rainfall recovery in West Africa. Int J Climatol 35:4589–4605

Sen PK (1968) Estimates of the regression coefficient based on Kendall's Tau. J Am Stat Assoc 63:1379–1389

Schneider U, Ziese M, Meyer-Christoffer A, Finger P, Rustemeier E, Becker A (2016) The new portfolio of global precipitation data products of the Global Precipitation Climatology Centre suitable to assess and quantify the global water cycle and resources. Proc Int Assoc Hydrol Sci 374: 29–34

Shongwe ME, van Oldenborgh GJ, van den Hurk B, van Aalst M (2011) Projected changes in mean and extreme precipitation in Africa under global warming. II. East Africa. J Clim 24:3718–3733

Sillmann J, Kharin VV, Zwiers FW, Zhang X, Bronaugh D (2013b) Climate extremes indices in the CMIP5 multimodel ensemble. Part 2: Future climate projections. J Geophys Res Atmos 118:2473–2493

Taylor KE (2001) Summarizing multiple aspects of model performance in a single diagram. J Geophys Res 106: 7183–7192

Taylor KE, Stouffer RJ, Meehl GA (2012) An overview of CMIP5 and the experiment design. Bull Am Meteorol Soc 93:485–498

Tomozeiu R, Agrillo G, Cacciamani C, Pavan V (2014) Statistically downscaled climate change projections of surface temperature over northern Italy for the periods 2021–2050 and 2070–2099. Nat Hazards 72:143–168

Wilks DS (1995) Statistical methods in the atmospheric sciences. Academic Press, San Diego, CA, p 64–93

Zhang X, Alexander L, Hegerl GC, Jones P and others (2011) Indices for monitoring changes in extremes based on daily temperature and precipitation data. Wiley Interdiscip Rev Clim Change 2:851–870

Zhang X, Hegerl G, Seneviratne S, Stewart R, Zwiers F, Alexander L (2014) WCRP Grand Challenge: Understanding and Predicting Weather and Climate Extremes. Tech Rep. World Climate Research Program. www.wcrp-climate.org/images/documents/grand_challenges/GC_Extremes_v2.pdf

Editorial responsibility: Eduardo Zorita, Geesthacht, Germany

Submitted: December 29, 2017; Accepted: June 19, 2018
Proofs received from author(s): August 15, 2018